Ellipsometric characterization of tungsten oxide thin films, before and after He plasma exposure

M. I. RUSU[1,*], Y. ADDAB[2], C. MARTIN[2], C. PARDANAUD[2], V. SAVU[1,*], I. I. LANCRANJAN[1], D. TENCIU[1]

[1]*National Institute of R&D for Optoelectronics INOE 2000, 409 Atomistilor, Magurele, PO Box MG-5, 77125, Ilfov, Romania*

[2]*Aix-Marseille Université, CNRS, PIIM UMR 7345, 13397, Marseille, France*

Thin films of WO_3 were grown by thermal oxidation on tungsten substrates at 400 °C, under 590 Torr oxygen pressure. Two of the WO_3 films were exposed to helium plasma, one at room temperature, and the other one at 400 °C. In order to determine and confirm the tungsten oxides thicknesses between 25 and 75 nm as previously estimated from Scanning Electron Microscopy (the cross-section of samples was prepared by Focused Ion Beam), ellipsometry measurements and modelling were performed. The specular reflectance spectra of the WO_3 thin films were acquired in the range 190-2100 nm, showing that the reflectivity of the films decreases with WO_3 layer thickness, especially at low wavelengths. It was observed that He exposed samples present lower values of refractive index and extinction coefficient compared to the unexposed sample.

(Received February 24, 2023; accepted April 7, 2023)

Keywords: Tungsten oxide, Thermal oxidation, Thin films, Ellipsometry characterization, Reflectance

1. Introduction

Spectroscopic ellipsometry (SE) is one of the most often chosen non-invasive techniques among many others [1], to investigate the optical properties. It has been used for detailed studies on tungsten oxide films made by different methods [2-13]. Also, along with the traditional methods, e.g. Scanning Electron Microscopy (SEM), Focused Ion Beam (FIB) cross-section, SE is a very efficient, highly sensitive, non-destructive technique used in estimating the thicknesses of the thin films from few angstroms to several nanometers, with an approx. 20 % error, and their optical constants [14].

Results of ellipsometry measurements refer to the sample as a whole. A subsequent evaluation by modelling of the measured data reveals that is necessary to extract properties of individual layers. Investigation of multilayer structures requires consideration of the properties of each layer. Building a good model involves knowledge of the sample structure: the substrate, the ordering and composition of layers (e.g. substrate/oxide/film1/film2/roughness), the dielectric function of the substrate, the roughness of the top-layer, the concentration of the contained voids etc. The more parameter values are unknown at the beginning of the evaluation, the more complex is the evaluation and eventually no analytical solution might be found if some unknown parameters to be defined are highly correlated. A possible solution for determining these parameters is step by step analysis of the sample during the preparation, by recording ellipsometry measurements after the growth of each individual layer. A more often used possibility of reducing the number of unknown parameters, more often used, consists in a number of results previously obtained from other techniques: Atomic Force Microscopy (AFM), SEM, UV-Vis spectroscopy, Raman spectroscopy, Fourier Transformer Infrared (FTIR) spectroscopy etc. [14-17].

This paper refers mainly to SE characterization (ellipsometry measurements, modelling and analyses) on WO_3 thin films with different thicknesses, obtained by thermal oxidation of polycrystalline tungsten substrates. Two of the samples were exposed to helium plasma, in order to fabricate thin WO_3 layers that mimic the possible oxidation of tungsten plasma facing components (PFCs) and to explore the effects on their properties. In future thermonuclear fusion devices Deuterium-Tritium (D-T) reaction will be operated with high release of energy, requiring PFCs to withstand the extreme environment. Owing to its favorable physical properties, tungsten is used for PFCs receiving highest fluxes in operating tokamaks and it will compose the ITER (International Thermonuclear Experimental Reactor) divertor [18-20]. The high temperature of PFCs (up to 1000 °C) associated with the possible presence of oxygen impurities or accidental scenarios (e.g. cooling system leakage, or an emergency shutdown of the divertor) may cause oxidation of the W-PFCs, whose surface properties would then be altered.

In this study, the ellipsometry measurements were performed in order to determine the thicknesses, the refractive indices n and the extinction coefficients k, and to analyze the reflectivity versus wavelength in 190-2100 nm domain for WO_3 thin films grown by thermal oxidation on tungsten substrates at 400 °C, under 590 Torr oxygen pressure, some of the samples being exposed to helium plasma post growth. Data from AFM topography

measurements, FIB cross-section, SEM, Transmission Electron Microscopy (TEM), Raman spectroscopy and X-ray diffraction (XRD) were previously recorded [21] and they are used with a great efficiency in building an accurate ellipsometry model of the tungsten oxide structures studied in this work. Also, in a previously paper [22], the diffuse reflectance spectra of these films were acquired in 2500-5500 nm range, by using a hemispheric reflectometer.

The experimental part is described in section 2 and the ellipsometry characterization of the tungsten oxide layers are detailed and discussed in section 3. Section 4 summarizes the conclusions of this study.

2. Experimental

WO_3 thin films were obtained by thermal oxidation of tungsten substrates. Polycrystalline recrystallized tungsten (pc-W) samples produced by A.L.M.T. Corp., Japan (purity of 99.99%), measuring 7×7×0.3 mm, were used as substrates. Firstly, all the samples were polished to a mirror-like surface, electro-polished, and cleaned in ultrasonic baths with acetone and ethanol. Then, in the oxidation process, the temperature was set at 400 °C, in order to be relevant for PFCs. The growth of WO_3 films by thermal oxidation of tungsten substrates and the conditions of their stability at 400 °C are described elsewhere [21, 22]. The oxidation processes were carried out under 590 Torr oxygen pressure. The idea was to be limited not by a low oxidation rate [21, 22]. The oxidation time was varied as it can be seen in the Table 1 (virgin tungsten (S1), 0.5 h (S2), 1 h (S3), 1.5 h (S4, S5, S6)). From the whole lot, the samples S5 and S6 were exposed to a low energy He plasma (~ 20 eV, 4×10^{21} m^{-2} fluency), with a flux of 2.5×10^{18} $m^{-2}s^{-1}$, at two different temperatures: room temperature (S5) and 400 °C (S6).

Table 1. Grain size, thickness and roughness of the studied samples obtained from SEM, TEM, FIB cross-section [20], and ellipsometry modeling

Sample	Oxidation process (Time/P_{O2}); He plasma exposure	SEM W Grain size [μm]	TEM $W0_3$ Grain size [nm]	FIB cross-section Thickness [nm]	Ellipsometry Thickness [nm]	Ellipsometry Roughness [nm]	MSE
S1	untreated	5-50	-	0	0	0.57±0.007	4.01
S2	0.5 h/590 Torr	-	10-30	~25	24.1±0.4	33±0.067	4.37
S3	1 h/590 Torr	-	10-30	~55	55.7±1	28±0.26	10.57
S4	1.5 h/590 Torr	-	10-30	~75	77.5±1.3	2.7±0.23	26.49
S5	1.5 h/590 Torr; He plasma exposed (room temperature)	-	10-30	~75	70.3±1.3	15±0.5	11.69
S6	1.5 h/590 Torr; He plasma exposed (400 °C)	-	10-30	~50	48.5±1.9	7.02±0.54	11.58

The ellipsometry measurements of WO_3 samples were performed with a UVISEL Ex-Situ System-HORIBA JOBIN YVON SA, equipped with a PMT (photomultiplier tube) detector that is highly sensitive in the visible and UV regions. For analysis in extended and near IR region, the instrument is equipped with a high sensitivity InGaAs detector with spectral responses reaching 2.1 microns. The sample is placed in a horizontal configuration. In order to achieve variable incidence angles, both the excitation and collection heads equally and simultaneously rotate around the sample (Fig. 1). The UVISEL data acquisition system allows capture rates up to 1 msec/point with excellent signal/noise ratio.

The ellipsometry measurements of the WO_3 films were performed from 190 to 2100 nm, with a 5 nm step (or 0.600 eV-6 500 eV range, with a 0.05 eV step), using an integration time of 200 msec. at 70º angle, in measurement configuration II: P – M = 45 [90]; M = 0 [90]; A = 45, where P is the polarizer, M is the modulator and A is the analyser [23].

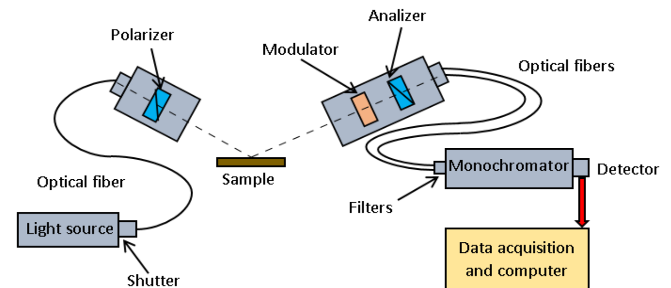

Fig. 1. The experimental set-up used in ellipsometry measurements

An ellipsometry model (Fig. 2) was created to determine the thicknesses and the roughness of the tungsten oxide films and to compare the results with those previously obtained from FIB cross-section and AFM [21]. The model used in this case is composed by two parts: the first one is simulated using the dielectric function of the studied material and the second one is simulated with an

Effective Medium Approximation (EMA) [24, 25]. The experimental data were fitted using the Bruggeman Effective Medium Approximation (BEMA) [26], taking into account the particularities of the oxidation method. The most used models describe the surface roughness of the studied sample with EMA. Many experimental comparisons have been made between EMA measured by ellipsometry and the morphology measured by AFM [25, 27]. Ref. [25] presents a review about the relationship between surface morphology and EMA roughness. After establishing the model, the appropriate dispersion function has been accounting for the materials in the sample, and the fit parameters were varied by least square regression until a minimum difference between experimental and computed (Ψ, Δ) spectra was obtained. The fit has been performed employing the dedicated software that automatically calculates the risk factor, using the mean squared error (MSE) and the appropriate regression function, to minimize the MSE function [28, 29]. Spectra of refractive indices (n) and extinction coefficient (k) for virgin tungsten substrate are plotted in Fig. 6, whilst the results obtained by spectroscopic ellipsometry are displayed in Table 1. Depending on the sample, the effective medium approximation uses a mixture between the dielectric function from the first part (m, a, b = 70 to 90 %) and the dielectric vacuum function for the void space presented in the harsh top-layer (q, z, d = 10 to 30 %). After establishing the layer thickness, the dielectric function of the material can be determined.

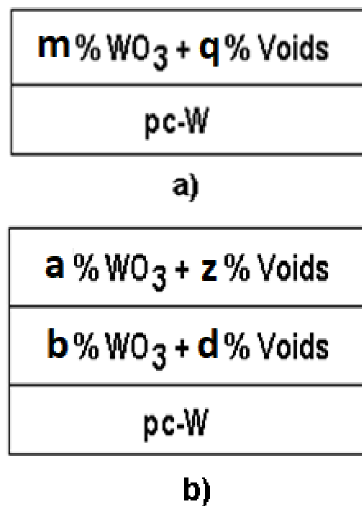

Fig. 2. The ellipsometry models created for the WO_3 thin films: a) m > n for films with thickness lower than 50 nm, and b) a < b and c > d for films with thickness higher than 50 nm

3. Results and discussion

The effects of the oxygen pressure, oxidation time and He plasma exposure on the structure and on the thickness of the WO_3 films, and their thermal stability in the 400 °C range were previously studied by Raman microscopy, XRD, SEM, TEM and AFM [21, 22]. The WO_3 films present, as expected, smooth surfaces with no cracks because of the low oxidation temperature. XRD results are specific for a monoclinic (m-WO_3) or orthorhombic (o-WO_3) nano-crystalline structure [21, 22]. Tungsten grain size measured by SEM is around 5-50 µm [21] and tungsten oxide grain size as obtained by TEM was found to be around 10-30 nm. The samples roughness measured by AFM was about 10 nm (not shown here).

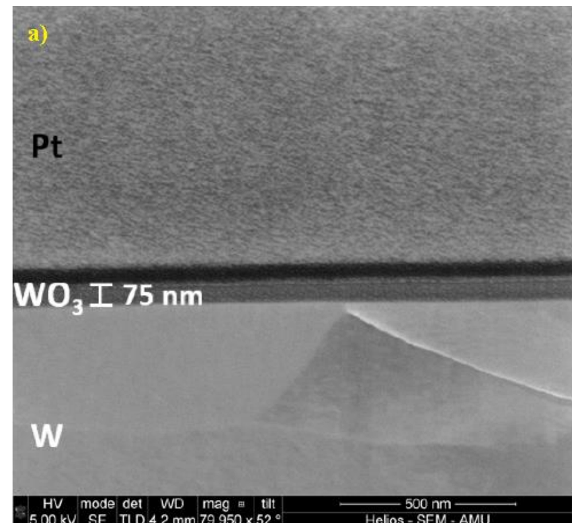

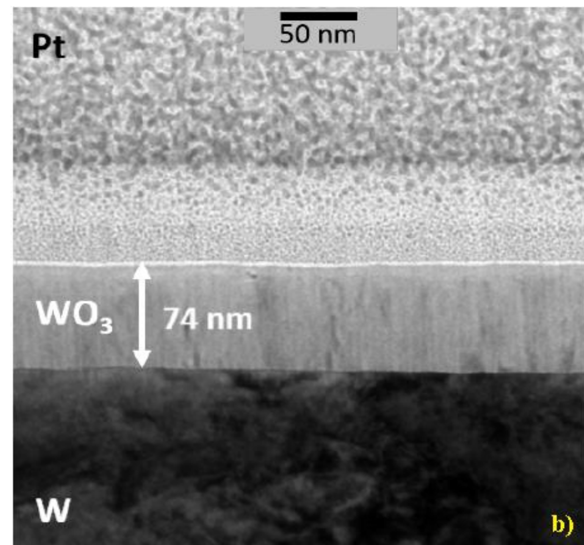

Fig. 3. a) SEM image of unexposed WO_3 sample (S4) and b) TEM image of room temperature He plasma exposed WO_3 (S5), prepared by FIB cross-section [21]

The results previously measured, as grain size, roughness and thickness, and those obtained by ellipsometry modelling are summarized in Table 1. Comparing the thickness and the roughness of the WO_3 films obtained by traditional methods, as FIB cross-section and AFM, with those determined from ellipsometry, it can be observed that the values are comparable with very small differences.

It is worth noting that S4 and S5 WO_3 films have similar FIB cross-section thickness (Fig. 3 and Table 1), around 75 nm, both films oxidized for 1.5 h, first of them

being unexposed and the second one being exposed to He plasma at room temperature. The thickness resulted from ellipsometry modelling are comparable with FIB cross-section thickness, being around 70 nm for both S4 and S5 WO_3 films. Thus, one can conclude that He plasma exposure at room temperature does not significantly influence the thickness of the WO_3 films and have no effect in terms of erosion on the surface of the oxide layer. For the room temperature He plasma exposed film (S5), the surface is smooth and the oxide/tungsten interface is well defined [21]. XRD and Raman analyses show that tungsten oxide layer after room temperature He plasma exposure remain crystalline (monoclinic nano-crystalline phase). This was expected as exposures were done at very low fluencies while such modifications were observed in Refs. [30-33] with much higher fluencies.

On the contrary, for the WO_3 film He plasma exposed at 400 ºC (S6), significant damages and formation of new features, as bubbles or void formations, at the tungsten oxide-tungsten substrate interface were revealed [21]. The oxide layer thickness in this case is measured at ~50 nm (measured by FIB cross-section and confirmed by ellipsometry –Table 1): a decrease in thickness of around 20 nm, which corresponds to an erosion rate of about 0.013 nm s^{-1}. Also, an about 10 nm deteriorated and low in oxygen WO_3 layer was observed at the surface of the film and nano-metric air bubbles were formed at the interface between oxide and tungsten substrate, due to the helium that crosses the oxide layer, this involving a decreasing of the reflection coefficient for WO_3 film. XRD measurements reveal that the WO_3 film after He exposure at 400 °C keeps the crystalline structure (monoclinic phase), but the quality of the films suffers damages (broken bonds, distortions of octahedra, additional tensions in the film structure) due to Raman analysis [21].

Fitting FIB cross-section thickness and ellipsometry thickness versus oxidation time (Fig. 4a), it can be observed the approximate linear increasing relation between them and the similarity of the fitting for the thickness obtained from FIB and ellipsometry. In the case of the samples exposed to He plasma, the graphs of thickness versus temperature during exposure (Fig. 4b) present a linear decreasing.

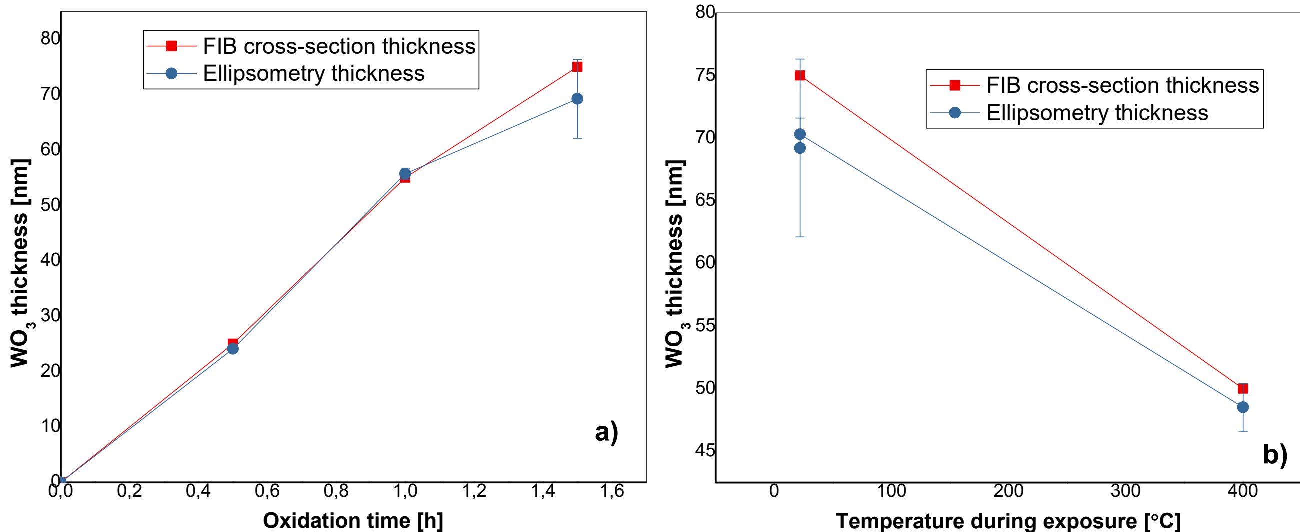

Fig. 4. FIB cross-section thickness and ellipsometry thickness (with error bar for ellipsometry thickness) versus a) oxidation time for unexposed WO_3 films, and b) versus temperature during exposure for He plasma exposed WO_3 films (color online)

The evolution of the specular reflection coefficient versus wavelength in the 190-2100 nm range was investigated, with the corresponding thickness and extinction wavelength as derived from the ellipsometry modelling. Fig. 5 presents the reflectance spectra for all five WO_3 films obtained by tungsten substrate annealing compared with virgin tungsten substrate. The shape of the reflectance curve is influenced by the thickness of the WO_3 film. As the thickness of the films decreases, the minimum of the reflectance is shifted to lower wavelengths. The reflectance spectrum of the virgin tungsten does not present a defined minimum. For all the samples, the reflectance is increasing in 800-2100 nm domain.

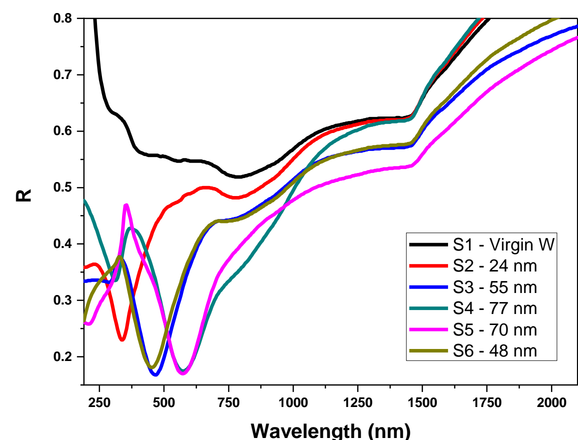

Fig. 5. The reflectance spectra of WO_3 films obtained on tungsten substrates compared with the reflectance of virgin tungsten substrate, in 190-2100 nm range (color online)

The refractive index *n* and extinction coefficient *k* obtained by modelling are compared with the ellipsometry measured ones. In Fig. 6 are shown the quite accurate overlaying of these parameters for virgin tungsten substrate. The overlaying procedure of *n* and *k* coefficients are successfully repeated for all the samples studied in this work (not shown here).

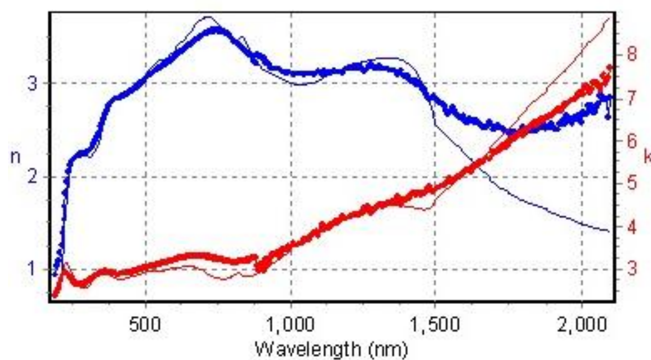

Fig. 6. Ellipsometry modelled n and k coefficients overlaid on measured n and k, for virgin tungsten substrate (color online)

Fig. 7 presents the refractive index and the extinction coefficient obtained by ellipsometry for one unexposed WO_3 thin film (S4) and for room temperature He plasma exposed WO_3 thin film (S5). There is an obvious changing in the optical properties of the tungsten oxide films after exposure to He. For unexposed WO_3 film, the absorption of the material increases from visible to infrared domain. On the contrary, for room temperature He plasma exposed WO_3 film, the absorption decreases in the same domain. Also, for unexposed WO_3 film it can be seen that the refractive index presents a minimum at 1000 nm, and in the case of room temperature He plasma exposed WO_3 film, the refractive index decreases beginning from around 400 nm to infrared domain.

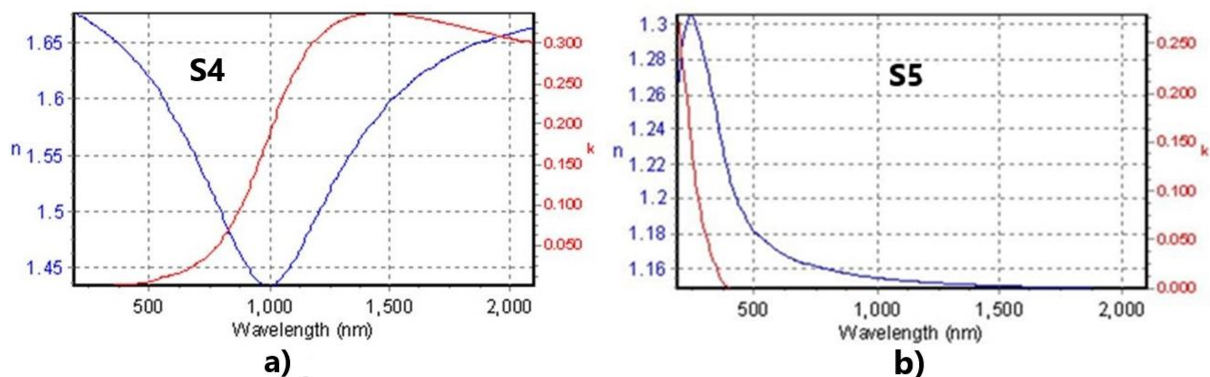

Fig. 7. Refractive index n and extinction coefficient k versus wavelength, resulted from ellipsometry measurements, for WO_3 films obtained after 1.5 h of oxidation. a) unexposed (S4), and b) room temperature He plasma exposed (S5) (color online)

4. Conclusions

Ellipsometry measurements were run on tungsten oxide films grown through thermal oxidation on tungsten substrates. Two of WO_3 films were exposed to helium plasma.

Models were created to determine the optical parameters, e.g. specular reflectance as a function of wavelength of the studied films. In the range 190 to 2100 nm the minimum of the reflectance is shifted to lower wavelengths as the thickness of the films decreases. The reflectance spectrum of the virgin tungsten does not present a sharp minimum, because the sample has no oxide films. For the oxide exposed to the He plasma, the n and k values are lower than those of the unexposed sample.

The *n* and *k* parameters were determined by for the virgin tungsten substrate and for WO_3 thin films for comparison. The modelled *n* and *k* versus wavelength were successfully overlaid to the *n* and *k* measured by ellipsometry, for all the samples studied in this paper. The values of these coefficients are higher for the unexposed WO_3 films than for He plasma exposed ones.

Acknowledgments

This research was funded by Core Program within the National Research Development and Innovation Plan 2022-2027, carried out with the support of MCID, project no. PN 23 05, the Romanian Ministry of Research, Innovation and Digitalization, through Program 1-Development of the national research-development system, Subprogram 1.2 - Institutional performance - Projects to finance the excellent RDI, Contract no. 18PFE/30.12.2021 and by the Romanian Ministry of European Investment and Projects & Romanian Ministry of Research, Innovation and Digitalization, contract no.8/1.2.1 PTI ap.2/17.02.2023.

References

[1] L. Ghervase, I. M. Cortea, R. Radvan, L. Ratoiu, A. Chelmus, Microchemical Journal **138**, 509 (2018).
[2] Y. Yamada, S. Kawaji, S. Bao, M. Okada, M. Tazawa, K. Yoshimura, A. Roos, Thin Solid Films **515**, 3825 (2007).
[3] Y. Yamada, K. Tajima, M. Okada, S. Bao, M. Tazawa, K. Yoshimura, A. Roos, Phys. Stat. Sol. C **5**(5), 1105 (2008).
[4] Y. Yamada, K. Tajima, S. Bao, M. Okada, K. Yoshimura, A. Roos, J. Appl. Phys. **103**, 1(063508) (2008).
[5] Y. Yamada, K. Tajima, S. Bao, M. Okada, K. Yoshimura, Solid State Ionics **180**, 659 (2009).
[6] I. Valyukh, S. Green, H. Arwin, G. A. Niklasson, E. Wackelgard, C. G. Granqvist, Solar Energy Materials & Solar Cells **94**, 724 (2010).
[7] I. Valyukh, S. Green, H. Arwin, G. A. Niklasson, E. Wäckelgård, C. G. Granqvist, Solar Energy Materials and Solar Cells **94**(5), 724 (2010).
[8] U. Kilic, A. Mock, D. Sekora, S. Gilbert, S. Valloppilly, G. Melendez, N. Ianno, M. Langell, E. Schubert, M. Schubert, Scientific Reports **10**, 10392 (2020).
[9] V. Ion, A. Andrei, M. Filipescu, F. Andrei, N. Enea, N. D. Scarisoreanu, M. Dinescu, Romanian Reports in Physics **73**, 507 (2021).
[10] H. Chen, A. Chiasera, S. Varas, O. Sayginer, C. Armellini, G. Speranza, R. Suriano, M. Ferrari, S. M. Pietralunga, Optical Materials: X **12**, 100093 (2021).
[11] M. Fried, R. Bogar, D. Takacs, Z. Labadi, Z. E. Horvath, Z. Zolnai, Nanomaterials **12**, 2421 (2022).
[12] K. B. Joël-Igor N'Djoré, M. Grafouté, Y. Makoudi, W. Hourani, C. Rousselot, Coatings **12**, 274 (2022).
[13] K. Ahmadi, International Journal of Scientific and Technical Research in Engineering (IJSTRE) www.ijstre.com **4**(5), 16 (2019).
[14] D. Lehmann, F. Seidel, D. R. T. Zahn, Springer Plus **3**, 82 (2014).
[15] T. Ivanova, A. Szekeres, M. Gartner, D. Gogova, K. A. Gesheva, Electrochimica Acta **46**, 2215 (2001).
[16] A. Szekeres, S. Alexandrova, P. Terziyska, M. Anastasescu, M. Stoica, M. Gartner, 21st International Summer School on Vacuum, Electron and Ion Technologies, Journal of Physics: Conference Series, IOP Publishing **1492**, 012056 (2020).
[17] M. Duta, M. Anastasescu, J. M. Calderon-Moreno, L. Predoana, S. Preda, M. Nicolescu, H. Stroescu, V. Bratan, I. Dascalu, E. Aperathitis, M. Modreanu, M. Zaharescu, M. Gartner, J. Mater. Sci.: Mater. Electron. **27**, 49132 (2016).
[18] F. Romanelli and JET EFDA Contributors, Nuclear Fusion **53**(10) 104002 (2013).
[19] S. Brezinsek and JET EFDA Contributors, J. Nucl. Mater. **463**, 11 (2015).
[20] S. Brezinsek, A. Widdowson, M. Mayer, V. Philipps, P. Baron-Wiechec, J. W. Coenen, K. Heinola, A. Huber, J. Likonen, P. Petersson, M. Rubel, M. F. Stamp, D. Borodin, J. P. Coad, A. G. Carrasco, A. Kirschner, S. Krat, K. Krieger, B. Lipschultz, Ch. Linsmeier, G. F. Matthews, K. Schmid and JET contributors, Nuclear Fusion **55**, 063021 (2015).
[21] H. Hijazi, Y. Addab, A. Maan, J. Duran, D. Donovan, C. Pardanaud, M. Ibrahim, M. Cabie, P. Roubin, C. Martin, J. Nucl. Mater. **484**, 91 (2017).
[22] Y. Addab, C. Martin, C. Pardanaud, J. Achkasov, D. Kogut, G. Cartry, G. Giacometti, M. Cabie, J. L. Gardarei, P. Roubin, Phys. Scr. **T167**, 014036 (2016).
[23] M. I. Rusu, Materiale nanostructurate pentru dispozitive optoelectronice: -Aplicații- Ed. Tehnopress, Iasi, Romania, pp: 1-230, (2019).
[24] B. Fodor, P. Kozma, S. Burger, M. Fried, P. Petrik, Thin Solid Films **617**, 20 (2016).
[25] A. Yanguas-Gil, H. Wormeester, Relationship between surface morphology and ef-fective medium roughness, in: M. Losurdo, K. Hingerl (Eds.), Ellipsometry at the Nanoscale, Springer, Berlin Heidelberg, Berlin, Heidelberg 179 (2013), http://dx.doi.org/10.1007/978-3-642-33956-1
[26] M. Khardani, M. Bouaïcha, B. Bessaïs, Phys. Stat. Sol. (c) **4**(6), 1986 (2007).
[27] S. J. Fang, W. Chen, T. Yamanaka, C. R. Helms, Appl. Phys. Lett. **68**, 2837 (1996).
[28] O. Toma, V. A. Antohe, A. M. Panaitescu, S. Iftimie, A. M. Raduta, A. Radu, L. Ion, S. Antohe, Nanomaterials **11**, 2841 (2021).
[29] M. I. Rusu, R. Savastru, D. Savastru, D. Tenciu, C. R. Iordanescu, I. D. Feraru, C. N. Zoita, R. Notonier, A. Tonetto, C. Chassigneux, O. Monnereau, L. Tortet, C. E. A. Grigorescu, Applied Surface Science, **248**, 950–955, (2013).
[30] A. Pezzoli, D. Dellasega, V. Russo, A. Gallo, P.A. Zeijlmans van Emmichoven, M. Passoni, J. Nucl. Mater. **463**, 1041e1044 (2015).
[31] V. K. Alimov, B. Tyburska, M. Balden, S. Lindig, J. Roth, K. Isobe, T. Yamanishi, J. Nucl. Mater. **409**, 27e32 (2011).
[32] S. Kajita, A. Ohta, T. Ishida, K. Makihara, T. Yoshida, N. Ohno, Jap. J. Appl. Phys. **54**, 126201 (2015).
[33] L. Baschir, D. Savastru, A. A. Popescu, I. C. Vasiliu, M. Filipescu, A. M. Iordache, M. Elisa, S. M. Iordache, O. Buiu, C. Obreja, J. Optoelectron. Adv. M. **21**(7-8), 524 (2019).

*Corresponding author: madalin@inoe.ro; savuv@inoe.ro